Journal of Hazardous Materials 174 (2010) 226–235

Contents lists available at ScienceDirect

Journal of Hazardous Materials

journal homepage: www.elsevier.com/locate/jhazmat

Floating boom performance under waves and currents

A. Castro[a,*], G. Iglesias[a], R. Carballo[a], J.A. Fraguela[b]

[a] Univ. of Santiago de Compostela, A. Hydraulic Eng., E.P.S., Campus Univ. s/n, 27002 Lugo, Spain
[b] Univ. of A Coruña, E.P.S., Campus de Esteiro s/n, Ferrol, Spain

ARTICLE INFO

Article history:
Received 24 June 2009
Received in revised form 7 September 2009
Accepted 8 September 2009
Available online 16 September 2009

Keywords:
Oil spill
Environmental damage
Floating boom
Physical model
Drainage failure

ABSTRACT

Floating booms constitute a fundamental tool for the protection of marine and coastal ecosystems against accidental oil spills. Their containment performances in exposed areas are often impaired by the action of waves, currents and winds in a manner which is dependent on the boom's response as a floating body, and which is not fully understood at present. In this work the relationship between the design parameters of a floating boom section and its efficiency against the mode of failure by drainage under a variety of wave and current combinations is investigated by means of physical modelling. Seven boom models with different geometries and buoyancy–weight ratios are tested with an experimental setup that allows them to heave and rotate freely. The model displacements under waves (both regular and irregular) and currents, as well as those of the free surface adjacent to the model, are measured with a Computer Vision system developed *ad hoc*. Two efficiency parameters are defined—the significant and minimum effective boom drafts—and applied to the results of an experimental campaign involving 315 laboratory tests. Thus, the manner in which the design parameters influence the boom's efficiency under different wave and current conditions is established.

© 2009 Elsevier B.V. All rights reserved.

1. Introduction

Oil spills resulting from maritime disasters have the potential to cause extensive environmental damage to the marine and coastal ecosystems. In spite of the safety enhancement measures recently implemented in oil transport by sea and the observed decrease both in the number of accidents and volume of oil spilled worldwide since 1970 [1,2], oil spills still constitute a significant risk. It is therefore not surprising that oil spill modelling is the subject of intensive research efforts (e.g. [3]). In order to reduce this risk it is important, first, to develop the ability to predict the path of an oil slick under the prevailing wind, wave and current conditions. A second issue of importance concerns the in situ response methods that may be used to deal with the oil slick on its approaching the coastline so that its environmental impact is as low as possible [4]. Mechanical methods, based on the use of floating booms to contain the oil slick and skimmers to recover the pollutant either from ships or the shoreline, are the most common countermeasure [5], among other reasons owing to a significant advantage over other methods (chemical dispersants, in situ burning, etc.)—the absence of adverse environmental effects. The success of mechanical methods hinges on the containment efficiency of floating booms. Though usually sufficient in sheltered waters, such as port basins or estuaries, it is often insufficient in open waters under the action of currents, waves and winds.

Among the various modes of failure of a containment boom, drainage failure—in which the contaminant escapes underneath the boom (Fig. 1)—is one of the most important. A crucial concept in this respect is the effective boom draft, or the draft available at a given moment considering the displacements of the free surface in the vicinity of the boom and those of the boom itself under the action of waves, currents and winds. Drainage failure occurs when the effective boom draft becomes lower than the oil slick thickness. The oil slick thickness depends on the characteristics of the particular oil spill (volume involved, hydrocarbon properties, etc.) and its evolution as determined by currents, winds, and waves (e.g. [6]). For this reason, unless focusing on a particular point in space and time during a particular oil spill, the oil slick thickness must be regarded as an unknown. Fortunately the other aspect of the problem (the effective boom draft) can be analysed in more general terms—and therein lies the motivation of this work.

The effective boom draft is a function of the geometry of the boom section and its motion, itself dependent on the hydrodynamic agents and the boom characteristics (geometry, buoyancy/weight ratio, etc.) In spite of the importance of boom motions, many previous works investigated drainage failure by means of fixed models, in most cases with highly simplified geometries (typically a vertical plate) and considering only the action of currents [7–10]. In these works, the boom draft was constant—undoubtedly a great simplification, though not a very realistic one. The draft reduction

* Corresponding author. Tel.: +34 982 28 59 00; fax: +34 982 28 59 26.
E-mail address: alberte.castro@usc.es (A. Castro).

0304-3894/$ – see front matter © 2009 Elsevier B.V. All rights reserved.
doi:10.1016/j.jhazmat.2009.09.040

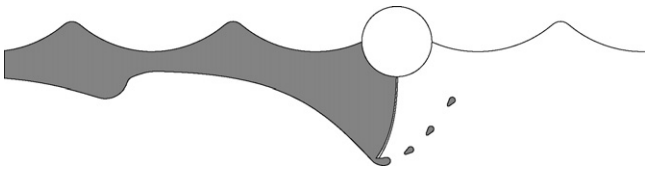

Fig. 1. Schematic of the mode of failure by drainage.

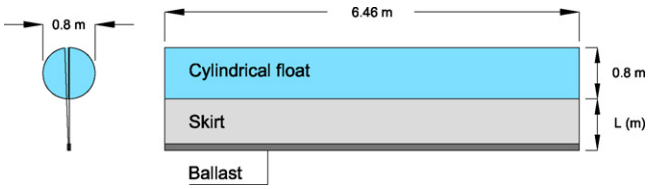

Fig. 2. Schematic of the reference boom module in prototype dimensions. The skirt length (L) may be 0.8 m or 1.2 m, depending on the model (see Table 1).

due to boom motions caused by wave action was investigated in a few works by means of numerical models based on the potential-flow assumption [11–13], generally taking into account the vertical displacement of the boom relative to the free surface, and also by means of laboratory experiments [13].

In this work the efficiency of seven boom section designs in relation to the mode of failure by drainage is investigated by means of realistic physical models that move vertically and rotate freely under the action of both waves and currents. For the reasons outlined above, allowing for these motions is crucial to a good assessment of the boom's performance. The motions are measured with a Computer Vision system based on the analysis of digital images. This system, designed *ad hoc* for this research [14], not only records the displacements of the floating model throughout each test, but also those of the free surface in its vicinity, which are necessary to determine the effective boom draft. The performance of the seven model booms is characterised by means of efficiency parameters based on the evolution of the effective boom draft during each test. These parameters, applied to an experimental campaign comprising, in total, 315 laboratory tests, enable to compare the performance of the different boom designs under various wave and current conditions and to analyse the influence of each design parameter on the boom's performance.

2. Materials and methods

2.1. Physical models

Seven physical models with different design sections were built at a 1:10 scale. The models represent a floating boom module with a length of 6.4 m, a buoyancy cylinder with a diameter of 0.80 m, and a vertical skirt with two possible heights: 0.80 m (models M1 to M4) and 1.20 m (models M5 to M7) (Fig. 2). The buoyancy cylinder was made of polystyrene and the vertical skirt was a PVC sheet. To achieve different values of the buoyancy–weight ratio (B/W), ballast was added in the form of stainless steel sheets attached to the bottom of the skirt—with the exception of the model M1, which had the largest B/W ratio. The ballast weight added to the remaining models was calculated so as to obtain three pairs of models with B/W ratios close to 15 (models M2 and M5), 10 (models M3 and M6) and 5 (models M4 and M7) respectively, each pair consisting of a short skirt and a long skirt model. In this manner the seven models present a range of variation both in initial draft (D_0) and B/W values which allows to analyse the influence of both parameters on the boom's performance. The main characteristics of the physical models are presented in Table 1.

2.2. Experimental setup

The physical tests were carried out in the wave and current flume of the University of Santiago de Compostela. The wave flume is 20 m long and 0.65 m wide with a maximum water depth of 0.8 m. Waves are generated by means of a piston-type paddle equipped with a system for absorbing reflected waves. At the opposite end of the flume, a wave-absorbing artificial beach with a slope ratio of 1:15 was used in order to minimise the effects on the model of the waves reflected at the end of the flume. The flume is also equipped with a reversible pumping system for current generation. The physical tests were performed with a water depth of 0.55 m. The physical model was placed at a distance of 10.3 m from the wave paddle (mid-position) and moored by means of four lines, 2.3 m in length, as shown in Fig. 3. Water surface elevation was measured by means of conventional wave gauges at five different stations along the longitudinal axis of the flume. A group of three sensors (WG_1, WG_2 and WG_3) was used to separate the incident and reflected waves by means of the method of Baquerizo [15]. They were placed between the wave paddle and the physical model at $x_1 = 8.0$ m, $x_2 = 8.8$ m and $x_3 = 9.1$ m respectively. The next wave gauge (WG_4) was located 25 cm in front of the physical model ($x_4 = 10.05$ m), while the last wave gauge (WG_5) was placed 25 cm behind the physical model ($x_5 = 10.55$ m) (Fig. 4).

2.3. Wave and current conditions

A total of 315 tests were conducted for as many combinations of waves and currents, using both regular and irregular waves. Three current velocities were used, 0 m/s, 0.257 m/s and 0.514 m/s (prototype values). In the regular wave tests wave heights were 0.25 m, 0.5 m and 1.0 m, and wave periods, 4 s, 6 s and 8 s; in the irregular wave tests the JONSWAP spectrum [16] was used, with four values of significant wave height (0.25 m, 0.5 m, 1.0 m and 1.25 m) and four values of the peak period (4 s, 6 s, 8 s and 10 s) (prototype values). Waves and currents were scaled according to the Froude model law, for the inertial forces are balanced primarily by the gravity forces—as is the case in most flows with a free surface [17]. With

Table 1
Parameters of the seven boom section designs (prototype values).

Boom parameter	M1	M2	M3	M4	M5	M6	M7
Cylinder diameter (m)	0.80	0.80	0.80	0.80	0.80	0.80	0.80
Skirt height (m)	0.80	0.80	0.80	0.80	1.20	1.20	1.20
Initial freeboard (m)	0.70	0.68	0.64	0.56	0.68	0.64	0.58
Initial draft (m)	0.90	0.92	0.96	1.04	1.32	1.36	1.42
Weight without ballast (N/m)	329.7	329.7	329.7	329.7	376.2	376.2	376.2
Ballast (N/m)	0.0	96.0	306.5	986.1	23.2	232.2	839.0
Total weight (N/m)	329.7	425.7	636.2	1315.8	397.8	608.4	1215.2
Desired B/W ratio	20	15	10	5	15	10	5
Actual B/W ratio	19.27	14.95	10.06	4.95	15.01	9.89	5.03
Centre of gravity (m)	0.67	0.86	1.09	1.28	0.89	1.25	1.57
Moment of inertia (Kg m)	6.9	14.2	35.3	94.2	17.3	54.5	150.0

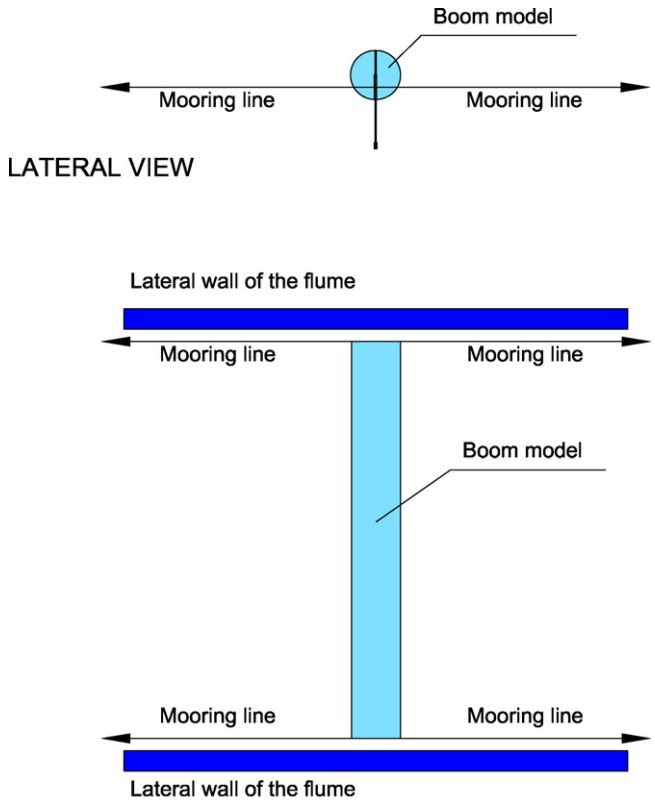

Fig. 3. Mooring arrangement in the laboratory flume.

a length scale ratio $N_l = 10$, the time and velocity scale ratios are $N_t = N_v = \sqrt{10}$.

2.4. Computer Vision system

A new Computer Vision system based on the analysis of digital images was developed *ad hoc* for measuring the model boom motions in a nonintrusive manner [14]. The system also provides the free surface elevation adjacent to the model boom—which is essential to determining the effective boom draft, itself a fundamental parameter for characterising boom behaviour. The Computer Vision system uses a set of processing algorithms to extract information from images recorded with a digital video camera. The camera is mounted on a tripod at a distance of 2 m from the flume sidewall, focusing the model section with its objective at the level of the quiescent water depth; it records a video sequence of the model section, which is subsequently processed by the Computer Vision system in order to determine the motions of the physical model and the free surface position. The former is obtained with the help of two identification marks (red squares) glued to the lateral of the buoyancy cylinder at symmetrical positions with respect to the vertical axis of the stationary model (in quiescent water) (Fig. 5). The system detects the marks in the image and draws a green line between their centres. By tracking this line,

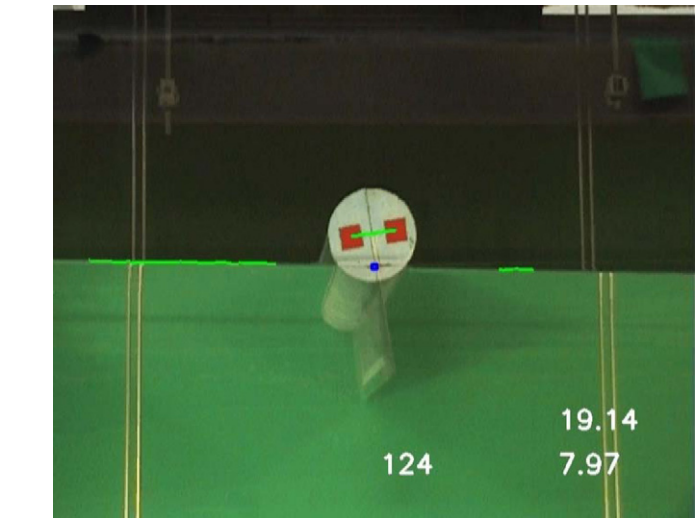

Fig. 5. Video frame after processing by the Computer Vision system. The model boom is at the centre, and the wave gauges WG_4 and WG_5 are on both sides. The numbers indicate the frame number (centre), the vertical coordinate of the float axis in mm (right, above) and the roll angle in degrees (right, below).

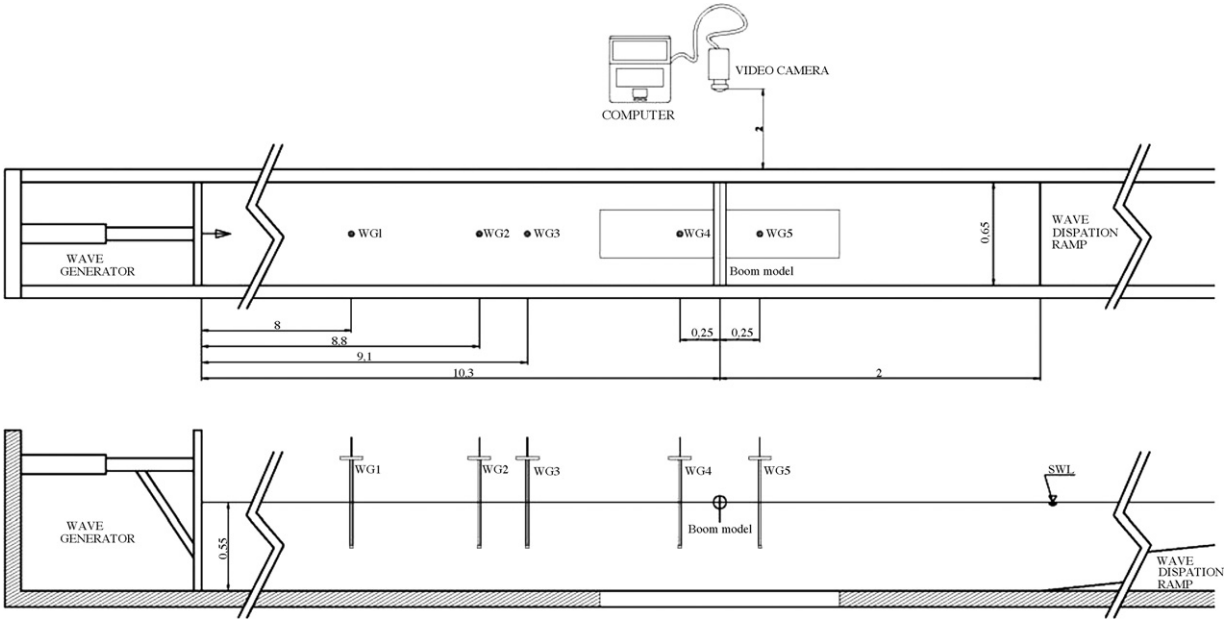

Fig. 4. Experimental setup showing the position of the model, wave gauges, wave generator, wave dissipation ramp, and video camera (distances in meters).

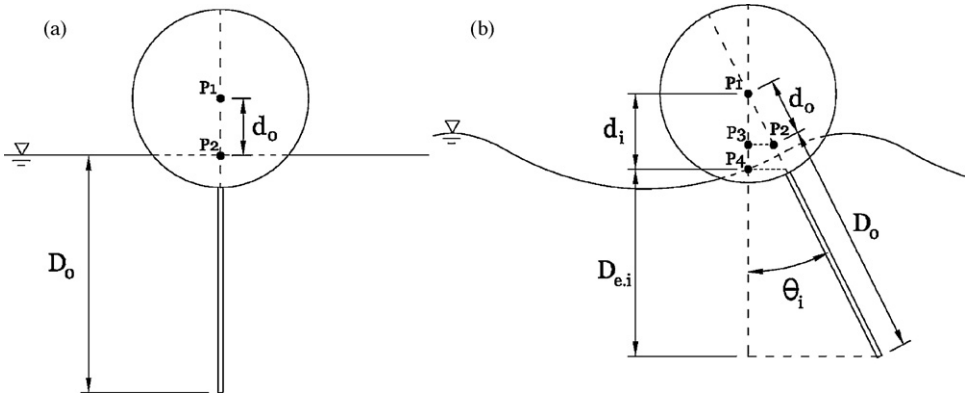

Fig. 6. Schematic of the model boom section at rest (a) and in motion (b). D_0, initial draft; $D_{e.i}$, instantaneous effective draft; θ_i, roll angle.

the system obtains the evolution of the boom's roll angle. Similarly, following the midpoint of the line—which coincides with the cylinder axis—the system obtains the model's vertical displacement. In order to detect the free surface position, a highly reflective green film was glued from the interior of the flume onto the opposite lateral wall. This film provided a back-lighting source for the water column, producing a high contrast between air and water in the digital images; the Computer Vision system detects the line separating the areas with different colours, i.e. the free surface.

2.5. Boom efficiency parameters

The concept of effective draft (D_e) was used to characterise the efficiency of the floating boom models due to its relationship with the drainage failure. The instantaneous values of this parameter ($D_{e.i}$) in the course of each test were obtained from the data provided by the Computer Vision system by means of the following expression:

$$D_{e.i} = (D_0 + d_0)\cos\ \theta_i - d_i, \tag{1}$$

where D_0 is the initial boom draft, d_0 is the vertical distance between the centre of the cylindrical float (P1) and the free surface position (P2) at rest (Fig. 6a), θ_i is the instantaneous roll angle of the model and d_i is the instantaneous vertical distance between the axis of the buoyancy cylinder (P1) and the free surface (P4) (Fig. 6b). Fig. 7 presents the evolution of the effective draft during one of the irregular wave tests. Once the instantaneous values of effective draft have been determined, two characteristic values are calculated: the significant effective draft ($D_{e.s}$) and minimum effective draft ($D_{e.m}$). These values allow to compare the efficiency of the different models under different wave and current conditions. The significant effective draft was calculated as the average of the one-third lowest local minima of the instantaneous effective draft values and was given by

$$D_{e.s} = \frac{1}{1/3}\sum_{j=1}^{1/3} D_{e.j}^{\min}, \tag{2}$$

where $D_{e.j}^{\min}$ are the local minima selected in ascending order and I is the total number of local minima. The significant effective draft provides a quantitative overall assessment of the boom behaviour during a given test in relation to drainage failure.

The minimum effective draft was given by

$$D_{e.m} = \min(D_{e.i}), \quad i = 1 \ldots I. \tag{3}$$

This value represents the least favourable situation in terms of effective draft (and hence of drainage failure) that occurred in the course of a given test.

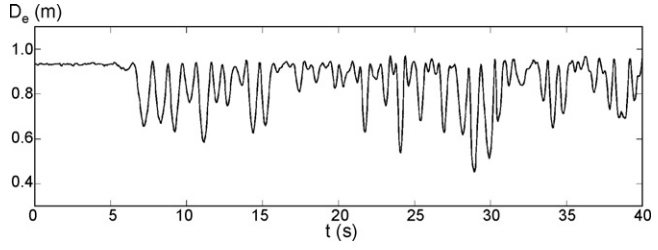

Fig. 7. Evolution of the effective boom draft during an irregular wave test of the M2 model. Test data: H_s = 1 m; T_p = 6 s; V_c = 0 m/s [Only the first part of the test is shown for clarity].

3. Results and discussion

The experimental results of significant and minimum effective draft obtained from the tests will be analysed separately for regular and irregular wave conditions. First, the general trends observed in the behaviour of the physical models as a function of the hydrodynamic conditions (current velocity, wave height and period) are commented. Next, the behaviour of the different models as a function of their respective design parameters (buoyancy–weight ratio and initial draft) is compared.

3.1. Regular waves

The results in terms of significant effective draft corresponding to the model M1 for the three values of current velocity tested (Fig. 8) show that this parameter decreases with increasing wave height or current velocity. Furthermore, the influence of wave height diminishes as the current velocity increases. Finally, the influence of the wave period is secondary. These general trends have been observed for all the physical models. With the objective of comparing the behaviour of the different models, the results obtained for all models with a wave period of 6 s are presented in Fig. 9. The values of the significant effective draft ($D_{e.s}$) are shown alongside those of the dimensionless significant effective draft ($D_{e.s}/D_0$). In the absence of current (Fig. 9a) the significant effective drafts of the long skirt models (M5, M6 and M7) are significantly larger than those of the short skirt models (M1, M2, M3 and M4) irrespective of the B/W ratio. On the other hand, considering separately each group of models, it is readily observed that the significant effective draft diminishes as the B/W ratio increases. When the model booms are subjected to both waves and a current (Fig. 9b and c) the significant effective draft diminishes as the current veloc-

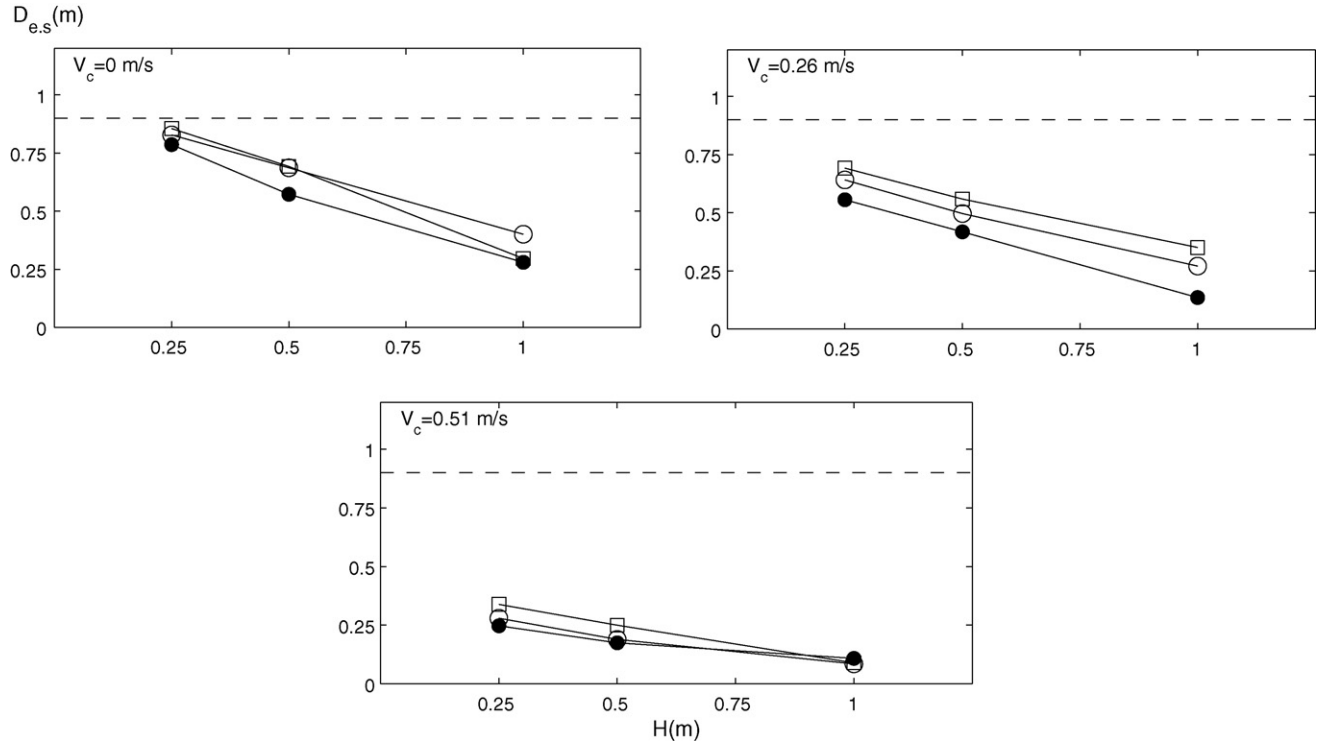

Fig. 8. Significant effective draft vs. wave height for three current velocities. Regular wave tests with the M1 model. [Initial draft (- - -); $T = 4$ s (□); $T = 6$ s (○); $T = 8$ s (●)].

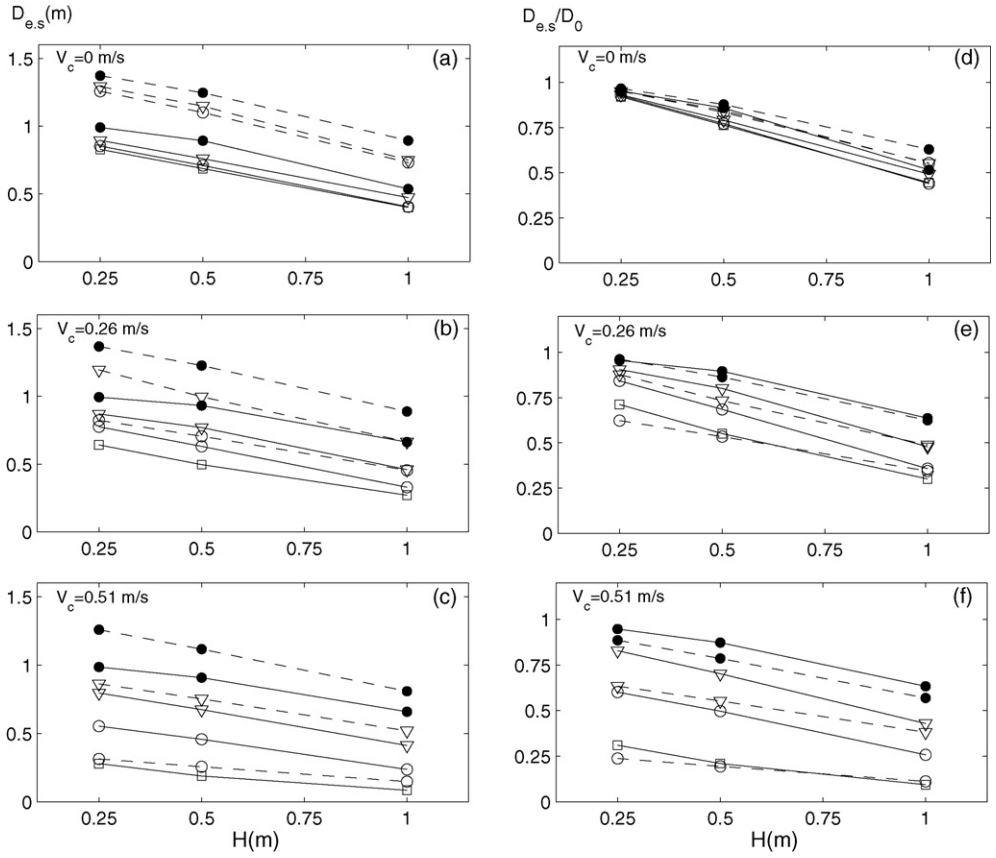

Fig. 9. Significant effective draft (left) and dimensionless significant effective draft (right) vs. wave height for three current velocities. Regular wave tests with $T = 6$ s. [Short skirt booms (––): M1 (□), M2 (○), M3 (▽), M4 (●). Long skirt booms (- - -): M5 (○), M6 (▽), M7 (●)].

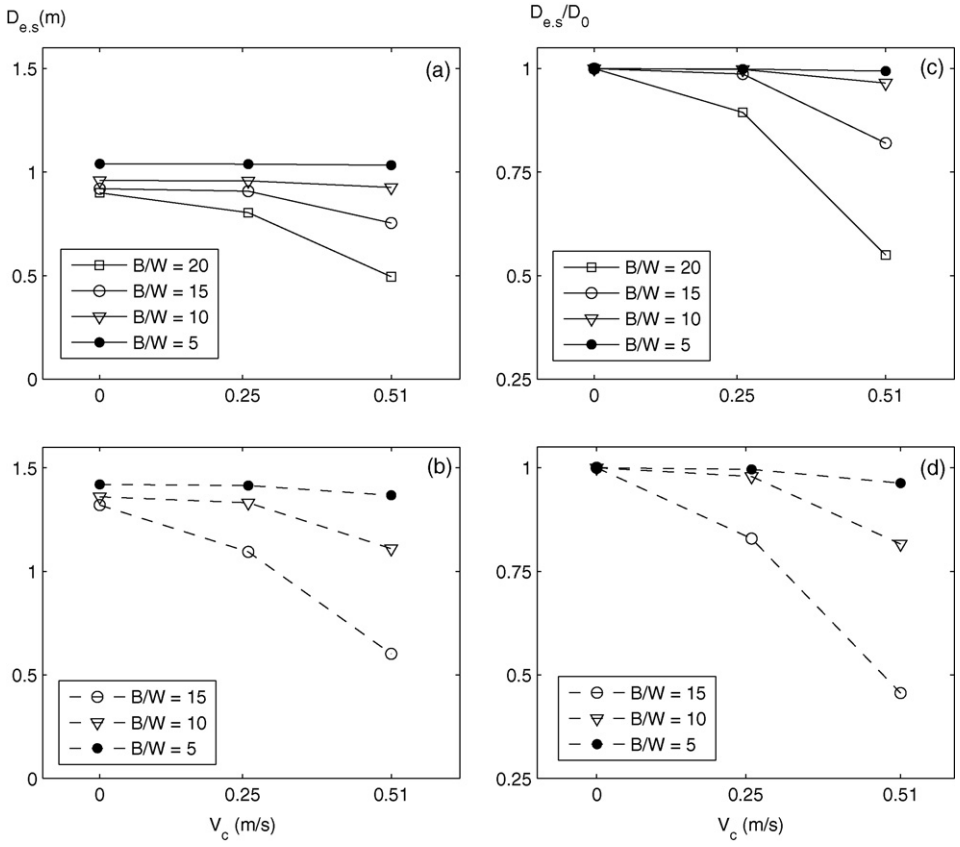

Fig. 10. Significant effective draft (a and b) and dimensionless significant effective draft (c and d) vs. current velocity for model booms with different B/W ratios, in the absence of waves. Above (a and c), short skirt models (––): M1 (□), M2 (○), M3 (▽), M4 (●). Below (b and d), long skirt models (- - -): M5 (○), M6 (▽), M7 (●).

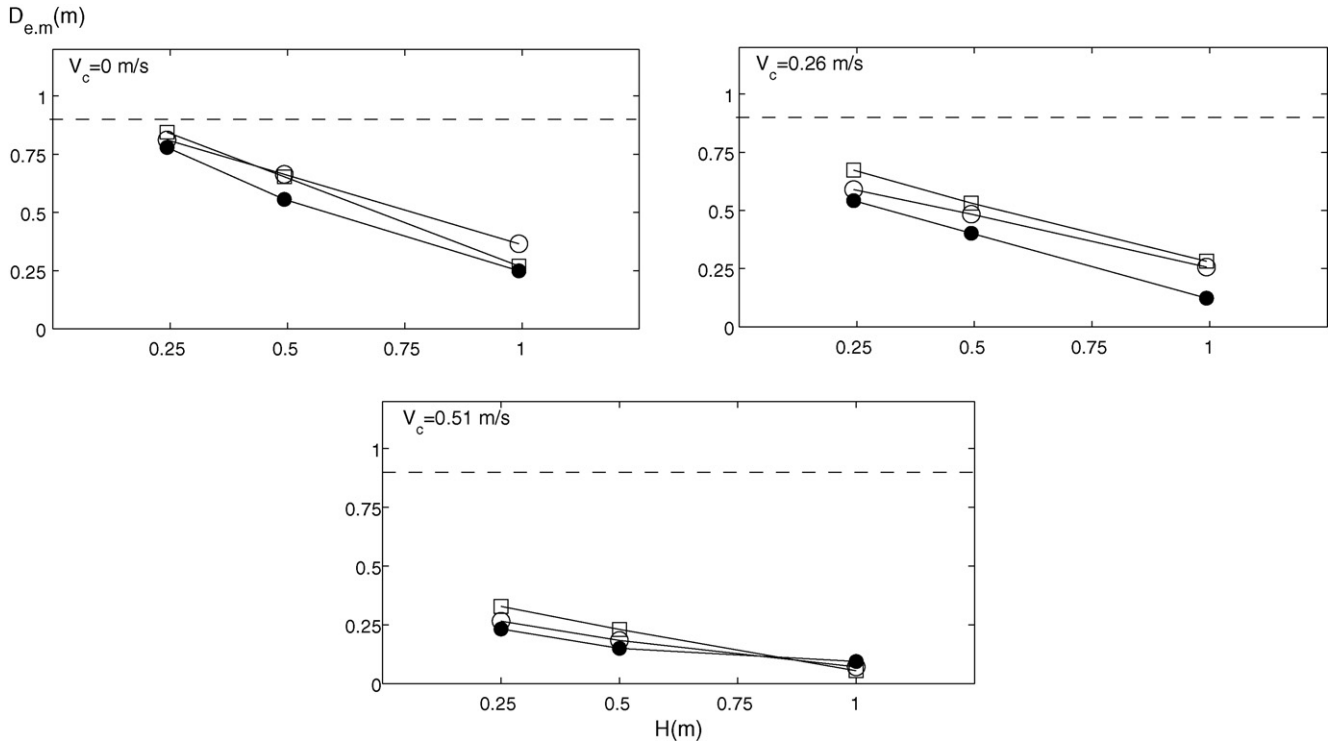

Fig. 11. Minimum effective draft vs. wave height for three current velocities. Regular wave tests with the M1 model. [Initial draft (- - -); $T = 4$ s (□); $T = 6$ s (○); $T = 8$ s (●)].

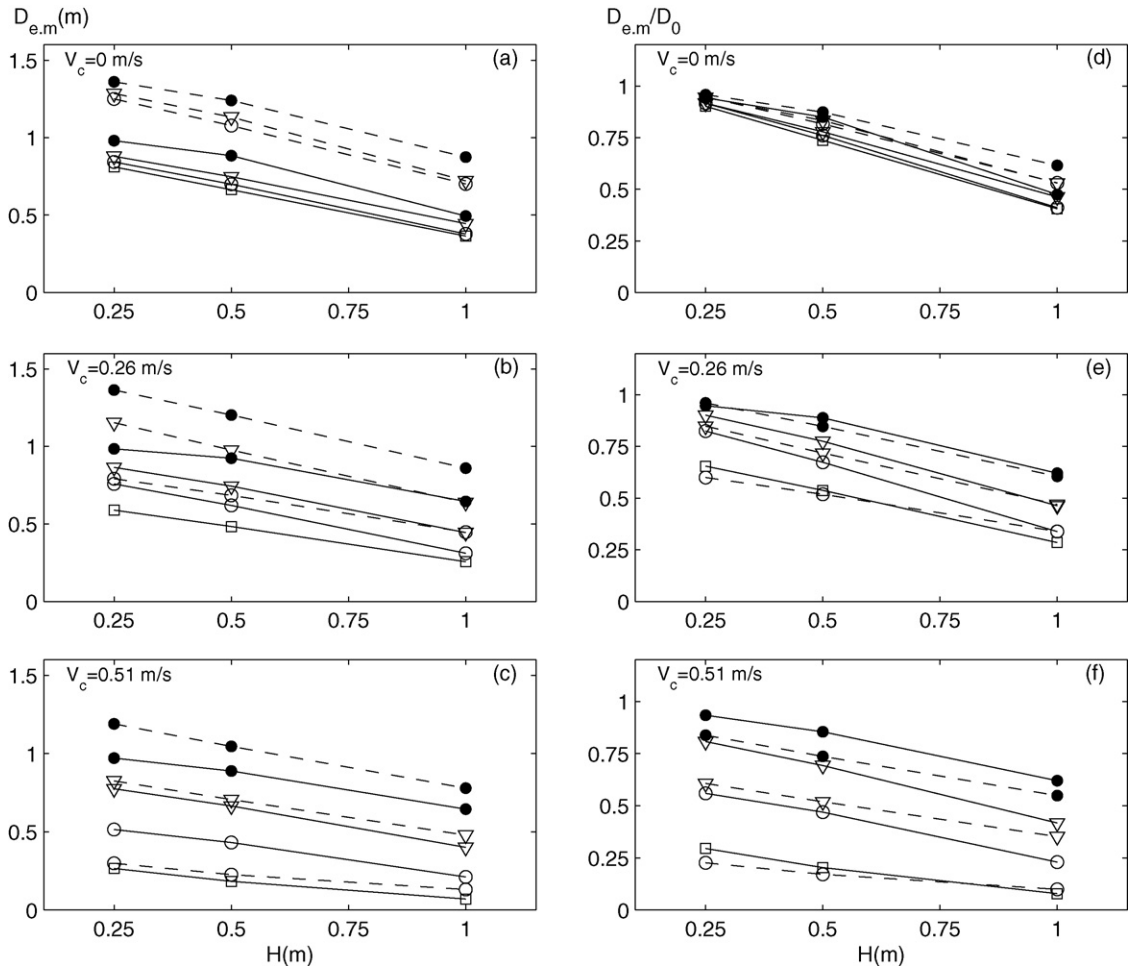

Fig. 12. Minimum effective draft (left) and dimensionless minimum effective draft (right) vs. wave height for three current velocities. Regular wave tests with $T = 6$ s. [Short skirt booms (––): M1 (□), M2 (○), M3 (▽), M4 (●). Long skirt booms (- - -): M5 (○), M6 (▽), M7 (●)].

ity increases. A further point of importance is the influence of the initial draft, i.e. of the skirt length. The effect of the current is more pronounced on the long skirt models (M5, M6 and M7) than on the short skirt models (M1, M2, M3 and M4), i.e. the former experience a greater reduction of effective draft as the current velocity is augmented. In the case of the models with a B/W ratio of 15, this effect is so pronounced that, for the strongest current (0.51 m/s), one of the long skirt models (M5) has a smaller significant effective draft than its short skirt counterpart (M2) (Fig. 9c).

The dimensionless significant effective draft is very informative as to the performances of the various boom designs. Beginning with the no current case, Fig. 9d shows that, for a given B/W ratio, the values of dimensionless significant effective draft obtained for the long skirt boom are larger than those corresponding to the corresponding short skirt boom. However, in the cases with both waves and current (Fig. 9e and f) the long skirt models present smaller values of the dimensionless significant effective draft—the current

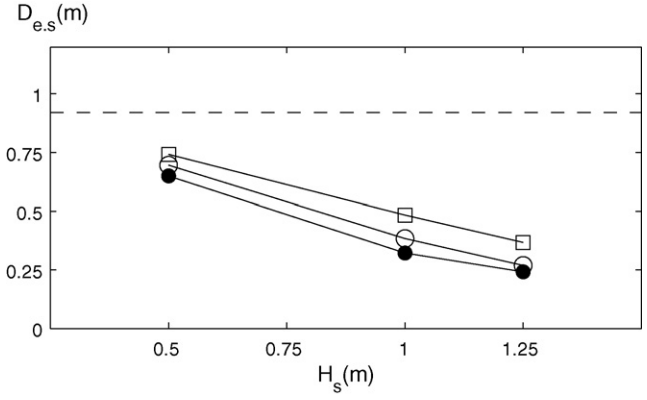

Fig. 13. Significant effective draft vs. significant wave height. Irregular wave tests with the M2 model. [Initial draft (- - -); $T_p = 6$ s (□); $T_p = 8$ s (○); $T_p = 10$ s (●)].

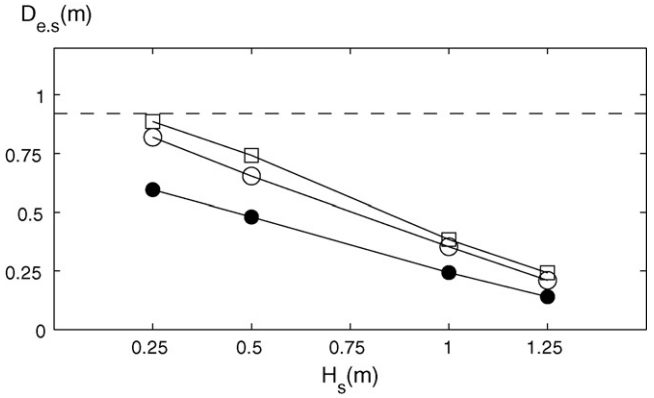

Fig. 14. Significant effective draft vs. significant wave height. Irregular waves with a current, M2 model. [Initial draft (- - -). Current velocities: $V_c = 0$ m/s (□); $V_c = 0.26$ m/s (○); $V_c = 0.51$ m/s (●). Wave conditions: ($H_s = 0.25$ m, $T_p = 4$ s); ($H_s = 0.5$ m, $T_p = 6$ s); ($H_s = 1.0$ m, $T_p = 8$ s); ($H_s = 1.25$ m, $T_p = 10$ s)].

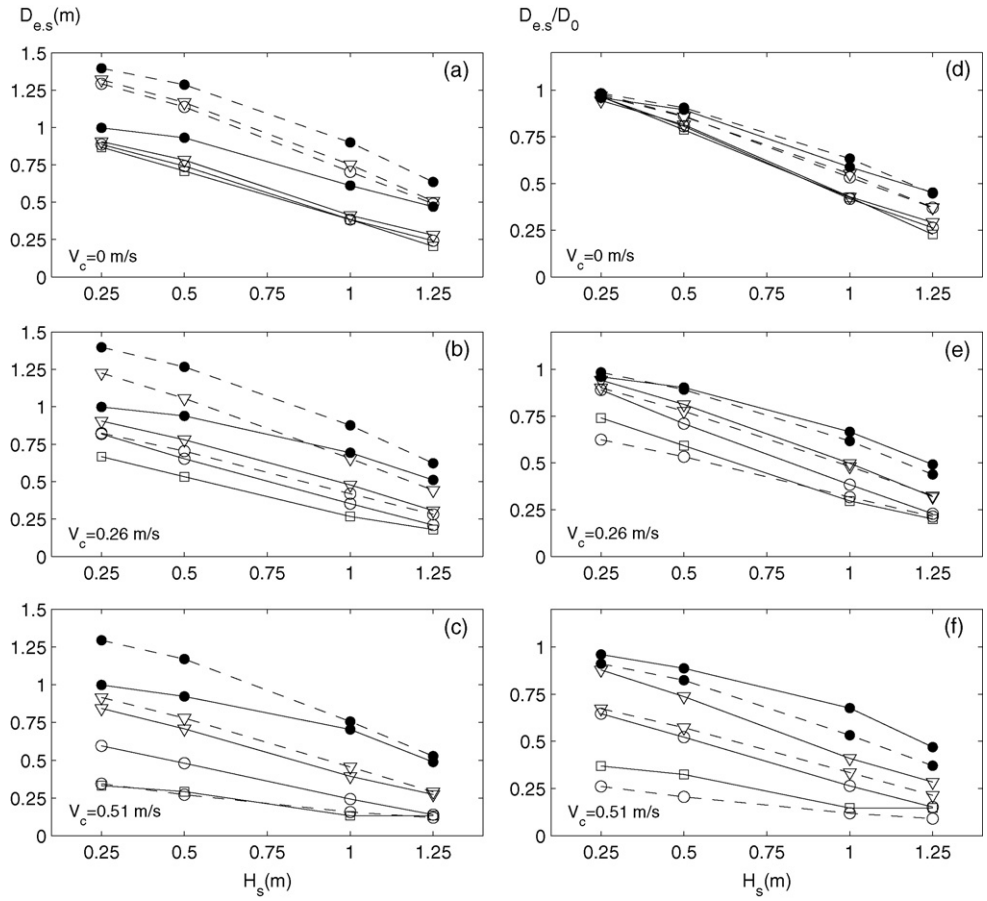

Fig. 15. Significant effective draft (left) and dimensionless significant effective draft (right) vs. significant wave height for three current velocities under irregular waves. [Short skirt models (––): M1 (□), M2 (○), M3 (▽), M4 (●). Long skirt models (- - -): M5 (○), M6 (▽), M7 (●). Wave conditions: (H_s = 0.25 m, T_p = 4 s); (H_s = 0.5 m, T_p = 6 s); (H_s = 1.0 m, T_p = 8 s); (H_s = 1.25 m, T_p = 10 s)].

generates a dynamic pressure on the skirt which causes the boom to roll, bringing about a draft reduction. For the same current velocity and B/W ratio, this effect is more marked with the long skirt boom. Naturally it increases as the current velocity, the B/W ratio, or both rise. The corollary is that increasing the skirt length does not necessarily result in a larger effective draft under current and waves, i.e. in a more effective boom design as regards the mode of failure by drainage.

The sensitivity to the current of model booms with different B/W ratios is compared in Fig. 10. It may be seen that, for a given current velocity, the models with a low B/W ratio (hereafter referred to for brevity as heavy models) experience, ceteris paribus, a lower reduction in either effective draft or dimensionless effective draft than their counterparts with higher B/W ratios (lighter models). At the limit, model booms with B/W = 5 (the smallest value used in the study) are hardly affected by the current. This is due to the fact that, for a given roll angle, the models with low B/W ratios experience larger righting moments than those with higher B/W ratios; and conversely, the righting moment necessary to balance the overturning moment caused by a given current velocity acting

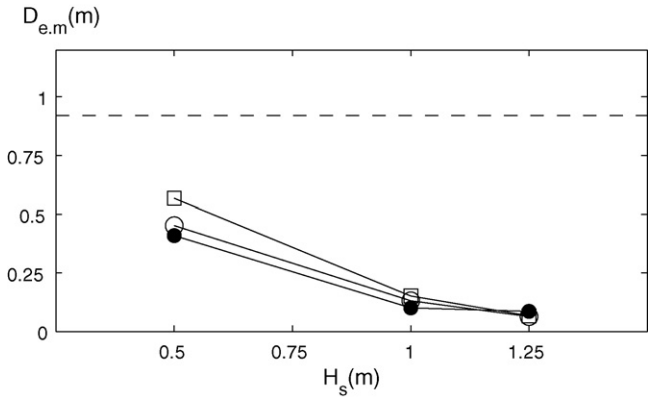

Fig. 16. Minimum effective draft vs. significant wave height. Irregular wave tests with the M2 model. [Initial draft (- - -); T_p = 6 s (□); T_p = 8 s (○); T_p = 10 s (●)].

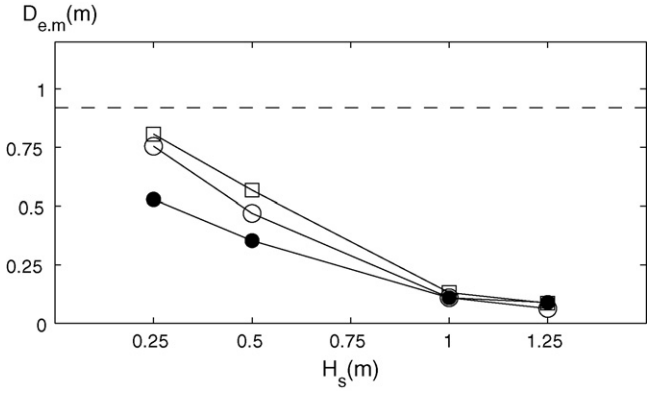

Fig. 17. Minimum effective draft vs. significant wave height. Irregular waves with a current, M2 model. [Initial draft (- - -). Current velocities: V_c = 0 m/s (□); V_c = 0.26 m/s (○); V_c = 0.51 m/s (●). Wave conditions: (H_s = 0.25 m, T_p = 4 s); (H_s = 0.5 m, T_p = 6 s); (H_s = 1.0 m, T_p = 8 s); (H_s = 1.25 m, T_p = 10 s)].

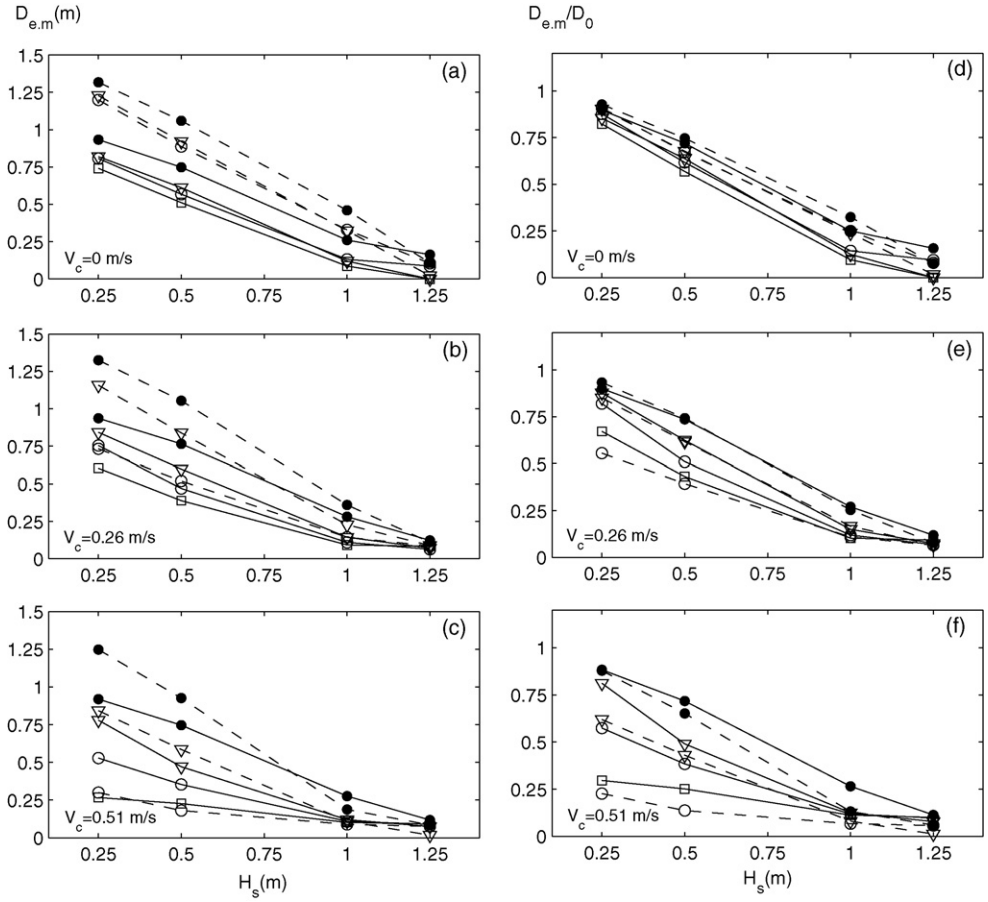

Fig. 18. Minimum effective draft (left) and dimensionless minimum effective draft (right) vs. significant wave height for three current velocities under irregular waves. [Short skirt booms (––): M1 (□), M2 (○), M3 (▽), M4 (●). Long skirt booms (- - -): M5 (○), M6 (▽), M7 (●). Wave conditions: (H_s = 0.25 m, T_p = 4 s); (H_s = 0.5 m, T_p = 6 s); (H_s = 1.0 m, T_p = 8 s); (H_s = 1.25 m, T_p = 10 s)].

on the boom is achieved with a smaller roll angle by the former. In other words, a given current velocity induces less roll, and hence a smaller draft reduction, in the models with a low B/W ratio than in their counterparts with higher B/W ratios, all other things being equal (in particular, skirt length). This is apparent in Fig. 10.

The results in terms of minimum effective draft for the M1 model (Fig. 11) show the same trends observed for the significant effective draft: the minimum effective draft diminishes as wave height, current velocity, or both rise; the influence of wave height decreases as the current velocity increases; and the influence of the wave period is secondary. Again these trends have been observed for all the physical models. In Fig. 12 the results in terms of minimum effective draft ($D_{e.m}$) and dimensionless minimum effective draft ($D_{e.m}/D_0$) obtained for all models with a wave period of 6 s are presented. It may be observed that the minimum effective draft follows similar trends to those of the significant effective draft.

3.2. Irregular waves

The results of the M2 model in terms of significant effective draft without and with a current are showed in Figs. 13 and 14, respectively. In the absence of a current the significant effective draft diminishes as the significant wave height increases; the influence of the peak period is secondary. In the presence of a current (Fig. 14), the significant effective draft decreases as the current velocity increases, and its value is overall less sensitive to the significant wave height. These trends have been observed with the seven model booms tested (Fig. 15). Comparing these results with those of the regular wave tests (Fig. 9) it is apparent that the influence of the B/W ratio and skirt length (i.e. initial draft) on the boom performances is similar under regular and irregular waves. The results of the M2 model in terms of minimum effective draft without and with a current are presented in Figs. 15 and 16, respectively. In the absence of a current, the influence of the significant wave height and the peak period follows the same lines observed for the significant effective draft (Fig. 13). In contrast, the effect of the current velocity (Fig. 17) depends on the significant wave height considered. For significant wave heights under 1 m, the minimum effective draft diminishes as the current velocity rises (as did the significant effective draft, Fig. 14). On the other hand, for significant wave heights above 1 m, the influence of the current velocity on the minimum effective draft is all but negligible.

The performances of the seven model booms are compared in Fig. 18 in terms of minimum effective draft and dimensionless minimum effective draft. It can be observed that, for $H_s \leq 1$ m, the variation of these parameters depends on the B/W ratio and the initial draft in much the same manner as did the significant effective draft. Notwithstanding, under the highest waves (H_s = 1.25 m), especially if acting alongside a current, the minimum effective draft becomes so small that the influence of either the B/W ratio or the initial draft vanishes.

4. Conclusions

Floating booms constitute a fundamental tool for the protection of marine and coastal ecosystems against accidental oil spills. Their containment efficiency in open water can be significantly impaired under currents, winds and waves. In spite of the great practical

importance of floating booms, our understanding of their response in the face of these hydrodynamic agents is still incomplete. In this work the performances of floating booms against the mode of failure by drainage under currents and waves (both regular and irregular) were investigated by means of physical modelling. Seven boom models with different geometries and buoyancy–weight ratios were tested under a large number of combinations of current velocity, wave height and period. In total, 315 laboratory tests were conducted.

Drainage failure is directly related to the concept of effective boom draft, itself a function of the displacements of the model and the free surface adjacent to it. Based on this concept, two statistical parameters were defined to assess the performances of the different boom designs: the significant effective draft and the minimum effective draft. Their values were computed for each test on the basis of the displacements of the model and the free surface in its vicinity, measured by means of a Computer Vision system developed *ad hoc* for this work.

As regards the hydrodynamic conditions, the higher the wave height or the current velocity, the smaller the significant and minimum effective drafts. The influence of the wave period was found to be secondary. The extent to which wave height and current velocity affect the boom's performances is intimately related to its design parameters, in particular its buyancy-weight (B/W) ratio and initial draft. For similar initial drafts, booms with high B/W values were found to be more sensitive to the hydrodynamic conditions (whether waves or currents) than those with low B/W values. In other words, for a given initial draft, a high B/W ratio results in less efficient designs.

As for the influence of the initial draft on the boom's efficiency, it is necessary to differentiate between two situations: a boom subjected only to wave action, or to both waves and currents. In the first case, the larger the initial draft, the better the containment performance. To analyse the second case, slightly more complex, the concept of dimensionless effective boom draft, or the ratio of the effective draft to the initial draft, was introduced. It was found that, for a given B/W value, boom sections with a long skirt experience a larger reduction of the dimensionless effective boom draft under waves and current than their short skirt counterparts. Furthermore, this effect becomes more pronounced as the current velocity, the B/W ratio, or both increase. The implication is that boom section designs with a larger initial draft can be, under certain conditions, less efficient against drainage than designs with a smaller initial draft. Owing to this somewhat counterintuitive fact, when a floating boom is to be deployed in an area where both waves and currents are present, the decision as to the most appropriate boom section design should be taken on the basis of physical model results (allowing for the model displacements as a floating body) or similar quantitative data, and considering the wave and current conditions expected.

Acknowledgements

This research has been funded by the European Union, within the framework of the Interreg IIIC programme (Ref. IIIA-PROLIT-SP1E194/03). The authors are grateful to two anonymous reviewers, whose suggestions and comments have contributed to improving the manuscript.

References

[1] P. Burgherr, In-depth analysis of accidental oil spills from tankers in the context of global spill trends from all sources, J. Hazard. Mater. 140 (2007) 245–256.
[2] D.R. Vieites, S. Nieto-Román, A. Palanca, X. Ferrer, M. Vences, European Atlantic: the hottest oil spill hotspot worldwide, Naturwissenschaften 91 (2004) 535–538.
[3] M. Fingas, B. Fieldhouse, Formation of water-in-oil emulsions and application to oil spill modelling, J. Hazard. Mater. 107 (2004) 37–50.
[4] D.F. McCay, J.J. Rowe, N. Whittier, S. Sankaranarayan, D.S. Etkin, Estimation of potential impacts and natural resource damages of oil, J. Hazard. Mater. 107 (2004) 11–25.
[5] N.P. Ventikos, E. Vergetis, H.N. Psaraftis, G. Triantafyllou, A high-level synthesis of oil spill response equipment and countermeasures, J. Hazard. Mater. 107 (2004) 51–58.
[6] R.H. Cross, D.P. Hoult, Oil booms in tidal currents, in: Proceedings of the 12th Coastal Engineering Conference, 1970, pp. 1745–1758.
[7] D.L. Wilkinson, Dynamics of contained oil slicks, J. Hydraul. Div. 98 (1972) 1013–1030.
[8] Y.L. Lau, J. Moir, Booms used for oil slick control, J. Environ. Eng. Div. 105 (1979) 369–382.
[9] B.L.J. Moloney, Oil spill containment using booms. MS Thesis, James Cook University, Townsville, Australia, 1996.
[10] J. Fang, K.-F. Wong, Instability of oil slicks contained by a single boom, in: Proceedings of the 23rd Arctic and Marine Oil Spill Program Technical Seminar, Environment Canada, Ottawa, 2000, pp. 447–468.
[11] I.-H. Cho, B.-W. Cho, Development of an optimal oil boom in wave, in: Proceedings of 14th International Oil Spill Conference, 1995, pp. 869–871.
[12] C.M. Lee, K.H. Kang, Prediction of oil boom performance in currents and waves, Spill Sci. Technol. Bull. 4 (4) (1997) 257–266.
[13] M.H. Kim, S. Muralidharan, S.T. Kee, R.P. Johnson, R.J. Seymour, Seakeeping performance of a containment boom section in random waves and current, Ocean Eng. 25 (2–3) (1998) 143–172.
[14] G. Iglesias, O. Ibáñez, A. Castro, J.R. Rabuñal, J. Dorado, Computer vision applied to wave flume measurements, Ocean Eng. 35 (2008) 1113–1120.
[15] A. Baquerizo, Wave reflection at beaches. Ph. D Thesis, University of Cantabria, Spain, 1995 (in Spanish).
[16] Y. Goda, Random Seas and Design of Maritime Structures, World Scientific, 2000.
[17] S.A. Hughes, Physical Models and Laboratory Techniques in Coastal Engineering, World Scientific, 1993.